Chapter 6

Spectroscopy of Ruthenium(II) and Rhodium(III) Intercalators Bound Noncovalently to DNA[‡]*

[‡]Adapted from: Franklin, S. J.; Treadway, C. R.; Barton, J. K.

Inorg. Chem. **1998**, *37*, 5198–5210.

*NMR spectroscopy and data analysis were performed by Dr. Sonya J. Franklin.

6.1 Introduction

Electron transfer mediated by DNA has recently been a subject of considerable interest and much controversy.[1,2] The oxidative quenching behavior of both covalently and noncovalently bound Ru(II) intercalators by Rh(III) intercalators with DNA has been shown by ultrafast emission and absorption spectroscopies to be exceedingly fast (>3 × 10^{10} s^{-1}).[3,4] Experiments in our laboratory have established that this rapid photoinduced quenching of ruthenium emission by bound rhodium is (1) the result of electron transfer rather than energy transfer,[5] (2) mediated by the DNA helix rather than solvent,[4] (3) sensitive to the intervening DNA sequence,[4] and (4) dependent upon strong intercalative stacking.[3,6–7] Photoinduced quenching of ethidium bound to DNA by rhodium intercalators proceeds similarly on a rapid timescale (>10^{9} s^{-1}).[8] Based in part upon these observations, we first proposed that the DNA double helix represents an efficient medium to facilitate long-range electron transfer.

Understanding whether and how the DNA helix might facilitate charge transport are important issues with respect to elucidating mechanisms for carcinogenesis and mutagenesis. Radiation biologists have debated whether radical migration through DNA occurs over 2 base pairs (bp) or 200.[9] With this perspective in mind, we also have carried out a range of experiments using covalently tethered intercalators to promote oxidative reactions in DNA from a remote site. In these investigations, we have observed oxidative damage to DNA arising over 30–40 Å using tethered rhodium(III)[10] or ruthenium(III) intercalators as the oxidant.[11] Additionally, we have demonstrated the oxidative repair of thymine dimers in DNA with a remotely positioned, covalently tethered intercalator.[12] As in the quenching studies, we have found that photoinduced charge transport is (1) mediated by the DNA base pair stack, (2) sensitive to the intervening DNA structure, and (3) dependent upon strong intercalative stacking. Moreover, in these assemblies the yield of oxidative damage or repair varies little with the distance separating the intercalator and site of oxidation. Experiments monitoring photoinduced quenching between covalently

tethered ethidium and rhodium in DNA assemblies have shown the quenching yield to be relatively insensitive to distance yet significantly dependent upon base pair stacking.[8] Indeed, our first experiment with tethered intercalator assemblies revealed rapid photoinduced quenching of ruthenium emission by a rhodium intercalator covalently bound at a separation of greater than 40 Å.[3]

Several researchers have proposed that the extremely fast quenching kinetics we have observed in the noncovalently bound Ru(II)/Rh(III) intercalator systems are due to the clustering of the metallointercalators on the DNA helix.[13,14] Such a cooperative association[15] would bring the complexes within close proximity of one another and would allow the observation of electron transfer rates which are fast compared to diffusion. The fast DNA-mediated electron transfer observed between ruthenium and rhodium intercalators differs substantively from electron transfer across proteins[16] and is inconsistent with expectations (based upon a theoretical study) of the electronic coupling in this system.[17] A study with nonintercalated yet coordinated reactants suggested electron transfer through DNA should be similar to that in proteins,[18] while a recent study[19] of photoinduced oxidation of guanine in a DNA hairpin by an associated (but unstacked) stilbene revealed an electronic coupling intermediate between that typical for a protein and that required to explain our observations with tethered intercalators.

Although this model represents an attractive explanation to some researchers, a clustering model is insufficient to explain the fast quenching we observe between tethered ruthenium and rhodium intercalators, and more generally the body of data that has since accrued on covalently modified assemblies. Moreover, the results obtained using noncovalently bound intercalators are fully consistent with those found using the covalently tethered assemblies. Additionally, a clustering model does not explain the sensitivity of the quenching observed with noncovalently bound intercalators to DNA sequence, and the lack of sensitivity to intercalator structure, symmetry, or hydrophobicity.[4,7]

In addition to modeling luminescence quenching titrations of noncovalently bound metallointercalators, one new experimental finding was put forth as evidence for the cooperative clustering of $[Ru(phen)_2dppz]^{2+}$ (phen = 1,10-phenanthroline, dppz = dipyridophenazine) and $[Rh(phi)_2bpy]^{3+}$ (phi = 9,10-phenanthrenequinone diimine, bpy = 2,2'-bipyridine) on the DNA duplex. Nordén and coworkers reported[13] that the circular dichroism (CD) for Δ-$[Ru(phen)_2dppz]^{2+}$ and Δ-$[Rh(phi)_2bpy]^{3+}$ bound to $[poly(dA\text{-}dT)]_2$ differs from the summation of the spectra for ruthenium bound to $[poly(dA\text{-}dT)]_2$ and rhodium bound to $[poly(dA\text{-}dT)]_2$ separately, and that this difference, an induced CD assigned to a cooperative interaction, is greater at a loading of 60 μM base pairs/(10 μM Ru + 10 μM Rh) compared to 250 μM base pairs/(10 μM Ru + 10 μM Rh). Neither the DNA sequence nor the concentrations of bound intercalators were varied systematically in the reported study, however.

Here we systematically reexamine these circular dichroism studies as a function of loading for three DNA polymers: $[poly(dA\text{-}dT)]_2$, mixed-sequence calf thymus DNA, and $[poly(dG\text{-}dC)]_2$. We previously observed fast quenching with all three DNA polymers, yet both the efficiency of photoinduced quenching and the rate of recombination (measured by transient absorption spectroscopy) decreased over the series $[poly(dA\text{-}dT)]_2 \geq$ mixed-sequence calf thymus DNA > $[poly(dG\text{-}dC)]_2$.[4] This more complete CD study does not support a clustering association of the two intercalators and instead establishes that the induced CD signal for each intercalator separately depends on DNA binding at moderate loadings. The study by Nordén and coworkers differed from those reported earlier in that they applied diastereomeric salts of the metallointercalators in titrations with DNA, and these may not have fully dissociated in solution, complicating their observations. Moreover, we present direct *structural* evidence for the noncooperative binding of the ruthenium and rhodium intercalators to a DNA decamer by NMR. Here we take advantage of the dramatic upfield shift of exchangeable imino protons in a DNA base pair upon intercalation to determine binding sites of the Rh(III)

and Ru(II) complexes on a DNA oligomeric duplex. The intercalators that we have studied, Δ-$[Rh(phi)_2bpy]^{3+}$ (Rh), Δ-$[Rh(phi)_2phen']^{3+}$ (Rh'), and Δ-$[Ru(phen)_2dppz]^{2+}$ (Ru), are shown in Figure 6.1. Dppz complexes of ruthenium(II) and phi complexes of rhodium(III) have been shown previously using NMR to bind DNA by intercalation in the major groove.[20,21]

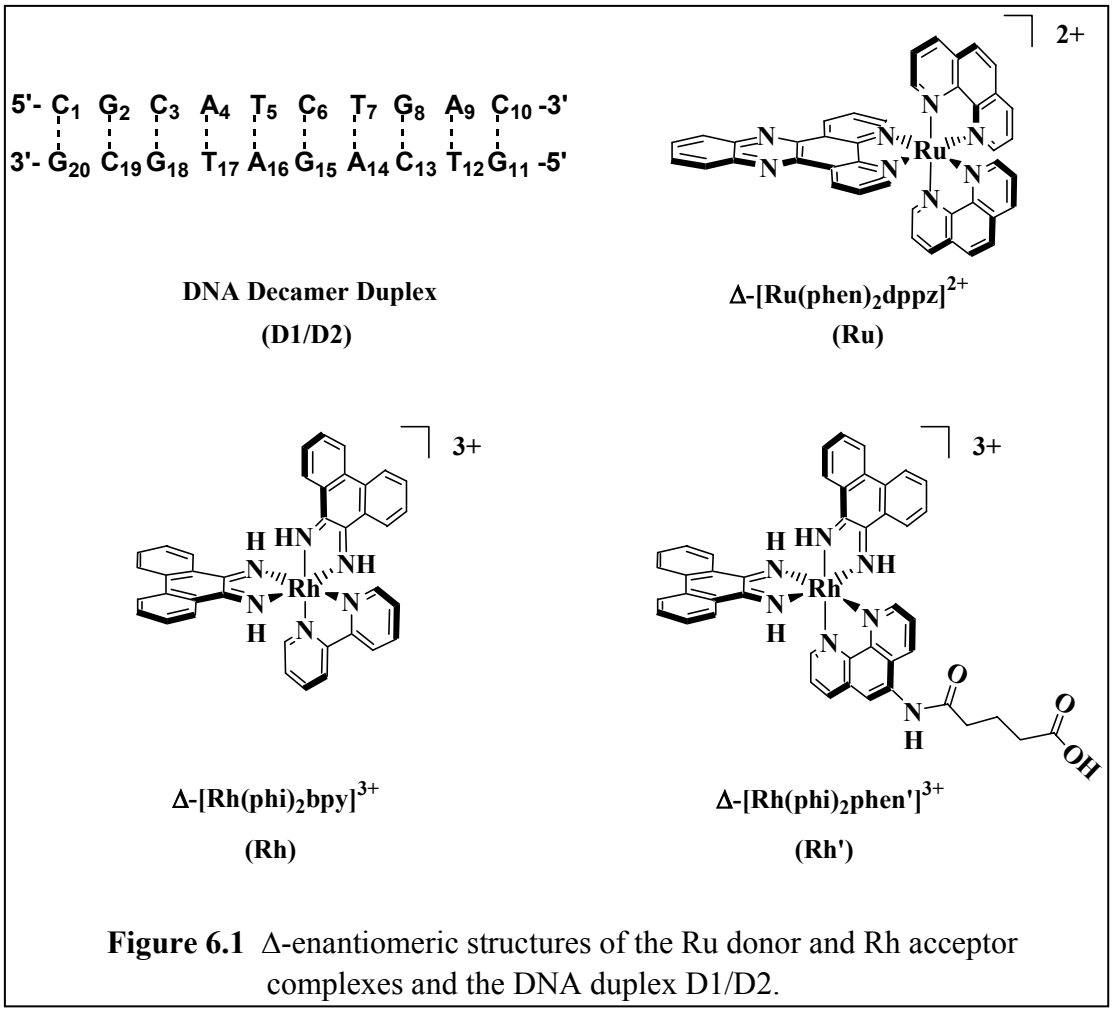

Figure 6.1 Δ-enantiomeric structures of the Ru donor and Rh acceptor complexes and the DNA duplex D1/D2.

6.2 Experimental Section

Materials. $[Ru(phen)_2dppz](PF_6)_2$ was prepared according to a modified procedure[22] and converted to the dichloride salt by anion exchange chromatography on Sephadex QAE-25 (Aldrich). $[Rh(phi)_2bpy]Cl_3$ and $[Rh(phi)_2phen']Cl_3$ were prepared as previously reported.[23] Trace impurities were removed by application of high pressure liquid chromatography (HPLC). Baseline resolution of Δ and Λ isomers from racemic mixtures was achieved chromatographically using a chiral eluant and standard methodology.[20,21,24,25] $[Poly(dA-dT)]_2$, $[poly(dG-dC)]_2$, and sonicated and phenol-extracted calf thymus DNA (Pharmacia) were exchanged into buffer (5 mM NaPi, 50 mM NaCl, pH 7.0) by ultrafiltration (Amicon). The single-strand decamers 5'-CGCATCTGAC-3' (D1) and 5'-GTCAGATGCG-3' (D2) were each synthesized on the 10 μmol scale and purified by HPLC; trityl protecting groups were removed, the strands were purified a second time by HPLC and desalted, and the triethylammonium cation from HPLC buffer was exchanged to sodium ion.

Instrumentation. CD spectra were recorded on a JASCO J-600 spectropolarimeter. UV-visible spectra were taken on either a Cary 2200 spectrophotometer or a Beckman DU 7400 spectrophotometer. Time-resolved fluorescence measurements on the nanosecond timescale were carried out using the facilities in the Beckman Institute Laser Resource Center, as has been described.[26] Excitation for nanosecond timescale emission studies was provided by an excimer-pumped dye laser (1.1 mJ/20 ns pulse at 10 Hz) containing Coumarin 480 (Exciton), with λ_{exc} = 480 nm and λ_{obs} = 610 nm. Steady-state emission from 500–799 nm was measured using an SLM 8000 spectrofluorometer with λ_{exc} = 480 nm. NMR spectra were acquired on a Varian Unity Plus 600 MHz spectrometer.

Methods. Circular Dichroism and UV-Visible Titrations. All CD experiments were performed at ambient temperature in aerated solutions in a pH=7 buffer of 5 mM NaPi and 50 mM NaCl. CD titrations were carried out in one of two ways. In the first

method, concentrated DNA (typically 5 mM bp) was added in aliquots to solutions containing Ru, Rh, or Ru+Rh (10 μM in each metal complex). This method was also used for UV-visible titrations. In the second method, concentrated Rh (0.4 mM) was titrated in aliquots into Ru/DNA solutions (10 μM Ru, 500 μM bp). All solutions were mixed thoroughly and allowed to equilibrate for 10 minutes before data collection. High-frequency noise was filtered out using JASCO J-600 software. The following extinction coefficients were used in quantitating solutions: Ru, 21,000 M^{-1} cm^{-1} at 440 nm; Rh and Rh', 23,600 M^{-1} cm^{-1} at 350 nm.

NMR Studies. DNA samples for NMR contained 0.5 mM D1/D2 duplex and 10 mM sodium phosphate, pH 7.0, in 90:10 H_2O/D_2O. The metal complexes Rh' and Ru were each titrated into a D1/D2 sample to a concentration of 0.45 mM. The 0.9:0.9:1 mixed-metal sample was prepared by titrating Rh' (0.45 mM) into the Ru/(D1/D2) sample.

Two-dimensional (2-D) NOESY spectra were acquired on a Varian Unity Plus 600 MHz spectrometer with a mixing time of 250 ms using Watergate gradient pulse water suppression[27] and analyzed using the program FELIX [Biosym Technologies/Molecular Simulations]. All spectra were recorded at 25 ˚C, except that for the free duplex, which was acquired at 10 ˚C. The spectra were referenced to HOD, taking variations in temperature into consideration.

Luminescence Studies. Time-resolved and steady-state emission studies on the nanosecond timescale were carried out at ambient temperature in aerated solutions in buffer at pH 7.2, 5 mM NaPi, 50 mM NaCl. Concentrations were 10 μM in each metal complex and 10 μM in D1/D2 DNA duplex. Individual data sets were the average of 400 shots. Data fitting was accomplished by the least-squares method of Marquardt using in-house (BILRC) software. Time-resolved emission quenching was quantitated by integration of the response-limited excited-state decays from 0–3 μs. Integrated steady-

state emission intensities were measured from 500–799 nm and compared to a 10 μM $[Ru(bpy)_3]^{2+}$ standard.

6.3 Results and Discussion

6.3.1 Circular dichroism

Titrations Monitored by Circular Dichroism. The observation reported[13] by Nordén and coworkers regarding a perturbation in the CD of Δ-$[Rh(phi)_2bpy]^{3+}$ and Δ-$[Ru(phen)_2dppz]^{2+}$ bound to $[poly(dA\text{-}dT)]_2$ at high loadings relative to the additive CD spectra of each bound to DNA individually prompted us to carry out a more extensive study of this phenomenon. No evidence for the cooperative binding of either complex to DNA had been obtained either by CD or other spectroscopic techniques,[28] and the energetic basis[14] proposed for such cooperativity (≥1 kcal) between different cationic intercalators seemed difficult to understand. These researchers reported very weak spectral differences at only two loadings, both substantially higher loadings than those used in studies of photoinduced electron transfer, and no systematic analysis of the trends or characteristics associated with the induced CD was noted. We therefore have investigated the CD behavior of these same complexes with various DNA sequences over a large range of metal:DNA ratios.

Spectra as a Function of Loading. Figure 6.2 shows the CD spectra obtained as a function of loading onto calf thymus DNA for Ru only, Rh only, and Ru+Rh (at a constant Ru/Rh ratio). As is evident in the Figure, the primary perturbation in the CD of each metal complex, and for both together, arises upon addition of the first aliquot of DNA. There is a substantial red shift in the CD associated with the first addition of DNA. We can also monitor binding of the metal complexes to the DNA in a titration by UV-visible spectroscopy. Based upon UV-visible hypochromism, each metal complex is in the bound form under these conditions. A change in CD for each intercalator bound within the chiral environment of the interbase pair site relative to free in solution is

expected. Indeed, for achiral intercalators, induced CD signals of this magnitude are routinely observed.[29]

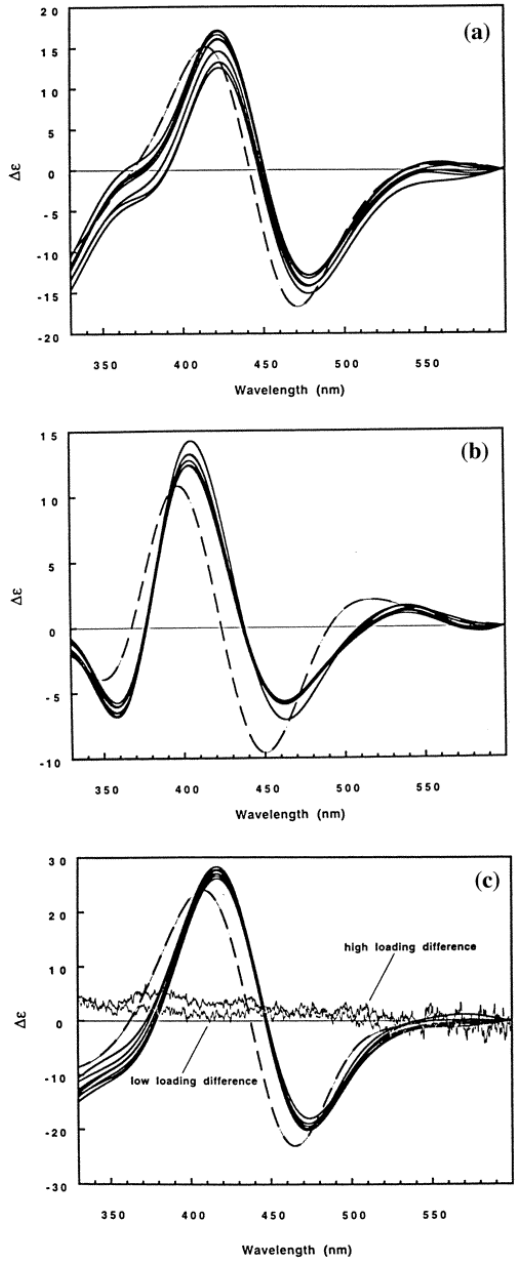

Figure 6.2 Circular dichroism of (a) Ru, (b) Rh, and (c) Ru+Rh in the absence (dashed) and presence (solid) of increasing calf thymus DNA concentration. Also shown in (c) are the difference spectra between Ru+Rh measured together versus the additive spectra of each separately at high loading (3 bp/metal) and at low loading (25 bp/metal).

Small variations in CD spectral intensity, on the order of the noise, are evident as a function of loading. For Ru only, as DNA is added, the CD signal intensity initially decreases, and thereafter the change is not systematic. For Rh only, the CD signal increases upon the first addition of DNA and then decreases. When Ru and Rh are present together, after an initial increase, the change is not systematic. Figure 6.2c also shows the difference spectra between Ru and Rh together and separately with DNA, at both high loading (comparable to Nordén's conditions) and low loading on the helix. *No spectral change is apparent for the complexes bound together to DNA versus independently bound.* If the metal complexes were to cluster on the helix, as proposed,[13] some spectral anomaly associated with their short-range interaction should be observed. Moreover, to be consistent with a clustering model, the spectral anomaly should be loading dependent. This is not what we observe. In fact, at the concentrations corresponding to that of low loading, ca. 50% of ruthenium luminescence is quenched on a rapid timescale with one equivalent of Δ-$[Rh(phi)_2bpy]^{3+}$.[7]

We examined the CD titration as a function of loading for $[poly(dA\text{-}dT)]_2$ and $[poly(dG\text{-}dC)]_2$ as well, and the results for the mixed-metal system are shown in Figure 6.3. Again, no systematic variation as a function of loading is apparent. It is noteworthy that significantly higher quenching efficiency was seen[4] with $[poly(dA\text{-}dT)]_2$ compared to $[poly(dG\text{-}dC)]_2$. Hence, a larger induced CD might be expected with the AT polymer. It is clear that the bound spectra differ in these two environments, but no systematic change occurs with loading. Moreover, the difference spectrum between the CD spectra for each metal bound together versus separately is at the level of noise at both loadings.

What is the source of the CD changes observed in the presence of DNA? They correlate most closely with variations in overall DNA binding by the metallointercalators as determined using UV-visible spectroscopy. Not surprisingly, the perturbation varies with respect to metal complex and DNA sequence. In one Ru+Rh titration ($[poly(dG\text{-}dC)]_2$) and some Ru-only titrations, initial addition of DNA causes a decrease in the CD

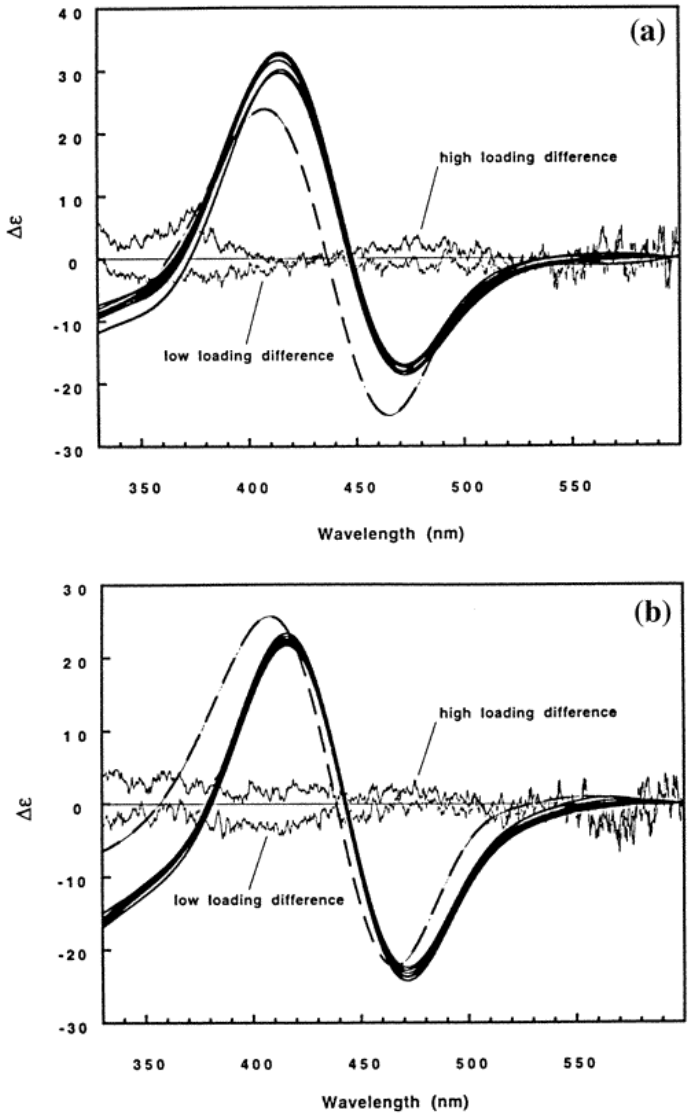

Figure 6.3 Circular dichroism of Ru+Rh in the absence (dashed) and presence (solid) of increasing concentrations of (a) $[poly(dA\text{-}dT)]_2$ and (b) $[poly(dG\text{-}dC)]_2$. Also shown are the difference spectra between Ru+Rh measured together versus the additive spectra of each separately at high loading (3 bp/metal) and at low loading (25 bp/metal).

signal intensity. In the titrations of Ru only and Ru+Rh with $[poly(dG\text{-}dC)]_2$, the intensity does not recover to its original level even after the nucleotide to metal complex ratio reaches 100:1. These observations parallel changes in hypochromicity observed by UV-visible spectroscopy. For Rh only, UV-visible titrations indicate that over this range of loadings, substantial hypochromicity is seen with the first addition of DNA with little change thereafter. Similarly, in the CD experiment, no systematic change in CD is evident after the first addition of DNA (all polymers) to Rh. The greatest binding is seen with Rh (to all polymers) while Ru binds more tightly to AT ≥ calf thymus > GC.[30] Our observations are consistent with spectral perturbations being the result of how well the complexes bind and intercalate into different polynucleotides. Similar changes in CD spectra of intercalators in the presence of DNA have been known since the 1960s.[29]

Can we reconcile our observations with those made by Nordén?[13] Our study encompasses a range of concentrations, an examination of how the CD changes for each metal complex separately and together, and different sequences. Hence, we may explore whether the very small variations observed by Nordén are systematic. They are not. In fact, under the condition of high loading described by Nordén, particularly with Rh present, we frequently observed changes in the UV-visible spectrum which are characteristic of precipitation; at this loading the metal complexes substantially neutralize the charge of the DNA polyanion. Evidence of kinetic precipitation at this loading was also found by following changes in the UV-visible absorption spectrum as a function of time or by varying the initial loading ratio in a titration.

The problem of precipitation is surely magnified as a result of the difference in sample preparation between our work and that reported by Nordén, and this difference may explain discrepancies introduced into their study. Titrations with DNA by Nordén were carried out using a diastereomeric arsenyl tartrate salt of Δ-$[Rh(phi)_2bpy]^{3+}$.[13,31] In all of our experiments, whether CD titrations, NMR studies, or electron transfer studies, diastereomers were first converted to the enantiomerically pure chloride salts by ion

exchange chromatography. In Nordén's study, presumably the assumption was made that the diastereomer dissociates in aqueous solution. However, the Rh CD spectrum in the presence of DNA reported[13] differs from that seen here with the pure enantiomer bound to DNA. Thus the arsenyl tartrate anion is clearly not fully dissociated in Nordén's experiment. The presence of the tightly held anion would certainly affect how the metallointercalators are distributed on the DNA helix.

Spectra as a Function of Rhodium. The CD as a function of increasing Rh was also examined, since it is under these conditions that photoinduced electron transfer studies have been reported.[4,7] As expected, the CD intensity increases with increasing Rh concentration. If the complexes were to bind cooperatively to DNA under these conditions, as proposed, we would expect[13] plots of CD intensity to increase nonlinearly as a function of Rh/Ru ratio. At higher ratios, in the context of a clustering model, more Ru should have Rh as a nearest neighbor, and a larger signal than that obtained from the simple addition of Ru and Rh spectra would be expected. In comparison to the quenching results, again, where ~50% quenching occurs with one equivalent Rh,[7] we would expect significant increases even with small additions of Rh. As shown in Figure 6.4, the change in the CD intensity with increasing Rh/Ru ratio in $[poly(dA\text{-}dT)]_2$ is inconsistent with the clustering model. If plotted as the CD intensity at the maximum absorption wavelength as a function of added Rh, the plot is strictly linear. If instead the signal intensity at 422 nm is plotted as a function of added Rh, the plot displays downward curvature at higher loadings, if anything, reflecting anticooperativity[15] at high binding ratios. Similar results were obtained with $[poly(dG\text{-}dC)]_2$ and calf thymus DNA.

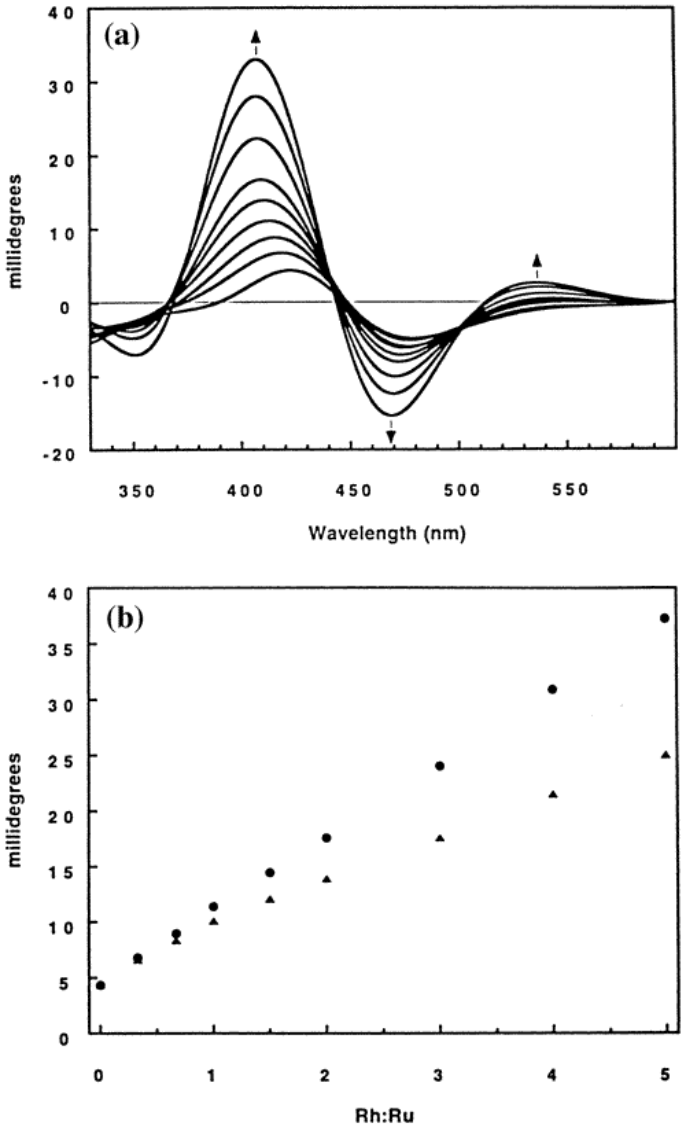

Figure 6.4 Circular dichroism of $[poly(dA\text{-}dT)]_2$ (0.5 mM bp) with Ru (10 μM) as a function of increasing concentration of Rh (0–50 μM) with spectra in (a) and data plotted in (b) as the CD intensity as a function of Rh:Ru concentration ratio at the CD maximum intensity wavelength (circles) and at 422 nm (triangles).

In summary, a more complete investigation shows that the CD data taken under conditions where fast, efficient quenching arise, do not support a cooperative mechanism for the binding of Ru(II) and Rh(III) cations to DNA. These data do not provide a "short circuiting" scheme to explain the fast photoinduced electron transfer observed between noncovalently bound intercalators.

6.3.2 NMR

NMR Study of Δ-[Ru(phen)$_2$dppz]$^{2+}$ and Δ-[Rh(phi)$_2$phen']$^{3+}$ Bound to a DNA Decamer. A far more direct structural picture of how the binding of the two intercalators to DNA influence one another is obtained using NMR. There are many challenges associated with applying NMR to this problem, however. Both complexes bind to DNA without high sequence selectivity, but a high-resolution NMR study requires single-site occupancy for the metal complex. Also, both metal complexes contain a plethora of aromatic protons; the overlap of these proton resonances with one another and with the DNA base protons can make assignments problematic. Well separated from the aromatic region of the spectrum in a 90:10 H_2O/D_2O solution, however, are the exchangeable imino protons associated with DNA base pairing.[32] These imino proton resonances characteristically exhibit upfield shifts of 0.5–1.0 ppm upon intercalation.[33] This upfield shifting has indeed been observed upon intercalation of both Ru(II) and Rh(III) complexes. This characteristic upfield shift may therefore be utilized in analyzing intercalation sites on DNA duplexes. The imine resonances of the DNA base pairs, in particular, are ideally suited to elucidate binding site, as (1) they are geometrically near the center of the helical axis, (2) there is only one imine resonance per base pair, and (3) their chemical shifts fall in an uncluttered region of the spectrum. Thus, by monitoring the upfield shift of imine peaks with intercalation, we can probe the binding sites of the metallointercalators individually or together.

We have studied Rh' and Ru together and each individually in the presence of a 10-mer oligonucleotide duplex. The carboxylate arm of the phen' ligand of Rh' does not

appreciably change the cleavage or quenching behavior (*vide infra*) of Rh' relative to Rh and allows us to explore a system closer in structure to the tethered complexes.[3,8,10,12] Moreover, the methylene protons provide a useful, well-separated marker for spectroscopic titrations. The 90:10 H_2O/D_2O spectrum of the non-self-complementary decamer, D1/D2 (5'-$C_1G_2C_3A_4T_5C_6T_7G_8A_9C_{10}$-3')/(5'-$G_{11}T_{12}C_{13}A_{14}G_{15}A_{16}T_{17}G_{18}C_{19}G_{20}$-3'), was fully assigned and characterized. The 0.9:1 metal/DNA spectra were then compared to that of the DNA alone. The spectra are remarkably well behaved, with intercalation occurring in slow exchange on the NMR timescale for the mixed-metal system. Given the exchange characteristics and obvious multiple-site occupancy for the metal complexes, a high-resolution structural determination is not possible from these data. However, the chemical shifts, exchange characteristics, and number of T and G imine peaks as well as cytosine NH_2 peaks may be used to assign and interpret the location of intercalating moieties in the DNA. This allows ascertation of the intercalation behavior of each metal alone and together. It is also important to note that although we looked for intermolecular NOESY cross-peaks between protons on the aromatic ligands of the metal complexes, the many proton resonances associated with these ancillary ligands are too difficult to deconvolute to be able to detect direct NOE interactions, if any exist. Figure 6.5 shows the two-dimensional (2-D) NOESY plots in the imine region for the DNA alone, Ru with DNA, Rh' with DNA, and mixed-metal/DNA system. The region of the 2-D spectrum containing cross-peaks due to C H5-H6 and C NH_2 is shown in Figure 6.6 for DNA alone, Rh'+DNA, Ru+DNA, and Rh'+Ru+DNA. These strong cytosine peaks serve as a characteristic fingerprint for the cytosine bases, and changes in this region reflect perturbations in chemical environment and exchange that arise with intercalation. Figure 6.7 shows the 1-D ^1H NMR spectrum in the imine region for the decamer with Ru only, Rh' only, and Ru+Rh'.

NOESY Contour for Rh'+DNA. With the addition of Rh', the DNA spectrum becomes significantly broadened compared to that of the DNA alone. The spectrum is

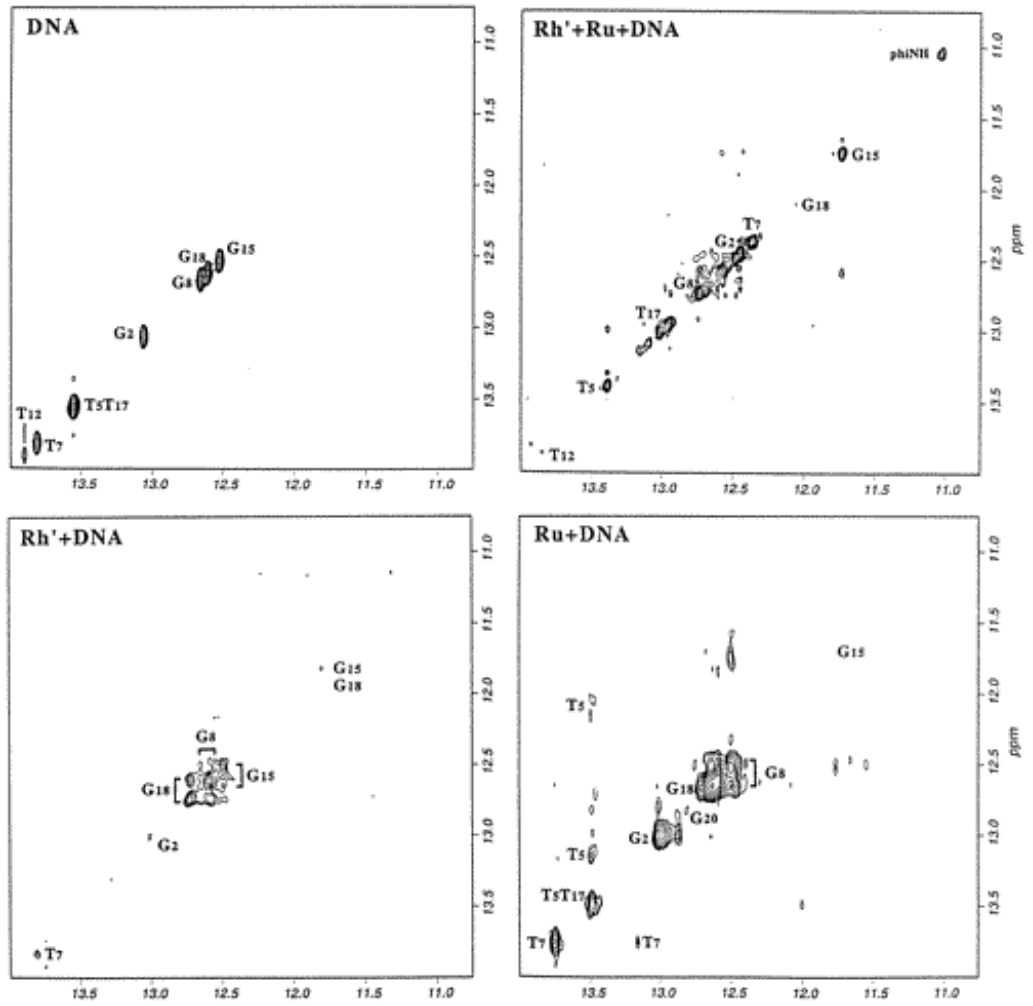

Figure 6.5 Expanded imine region of the 2-D NOESY Contours in 90:10 H_2O/D_2O for (counterclockwise from top left) D1/D2 alone, Rh'+D1/D2, Ru+D1/D2, and Rh'+Ru+D1/D2.

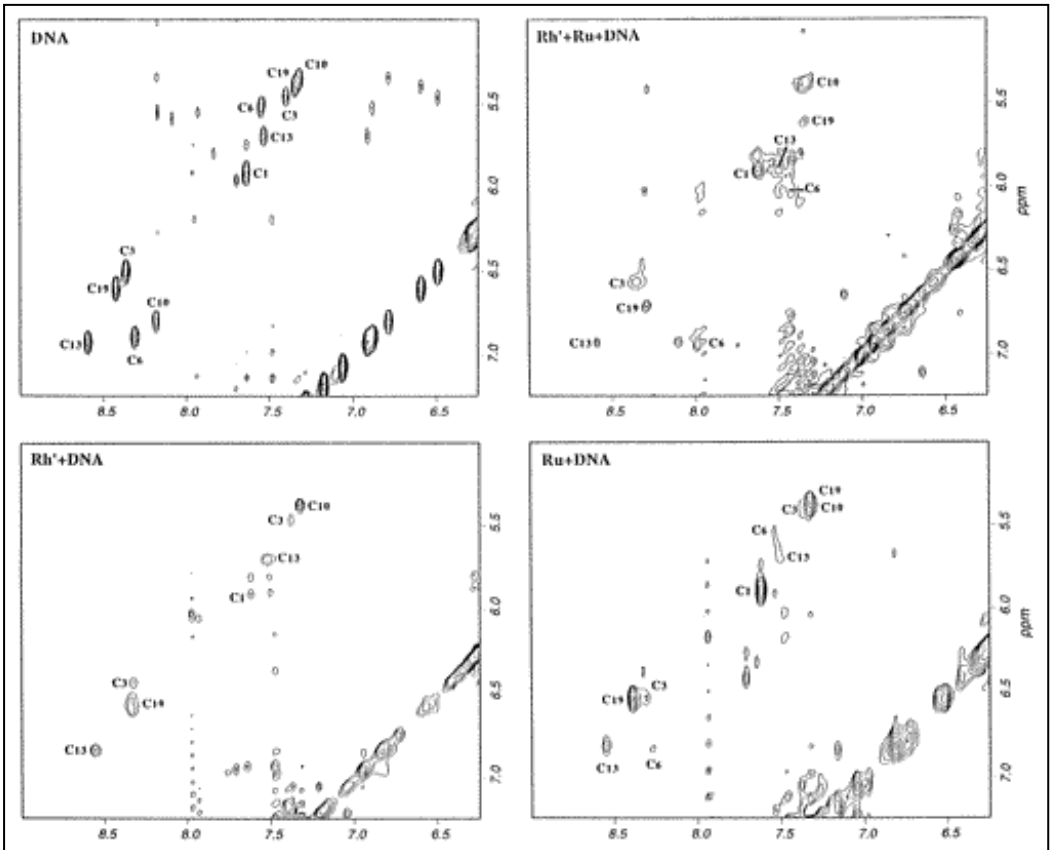

Figure 6.6 Expanded cytosine fingerprint region of the 2-D NOESY Contour in 90:10 H_2O/D_2O for (counterclockwise from top left) D1/D2 alone, Rh'+D1/D2, Ru+D1/D2, and Rh'+Ru+D1/D2.

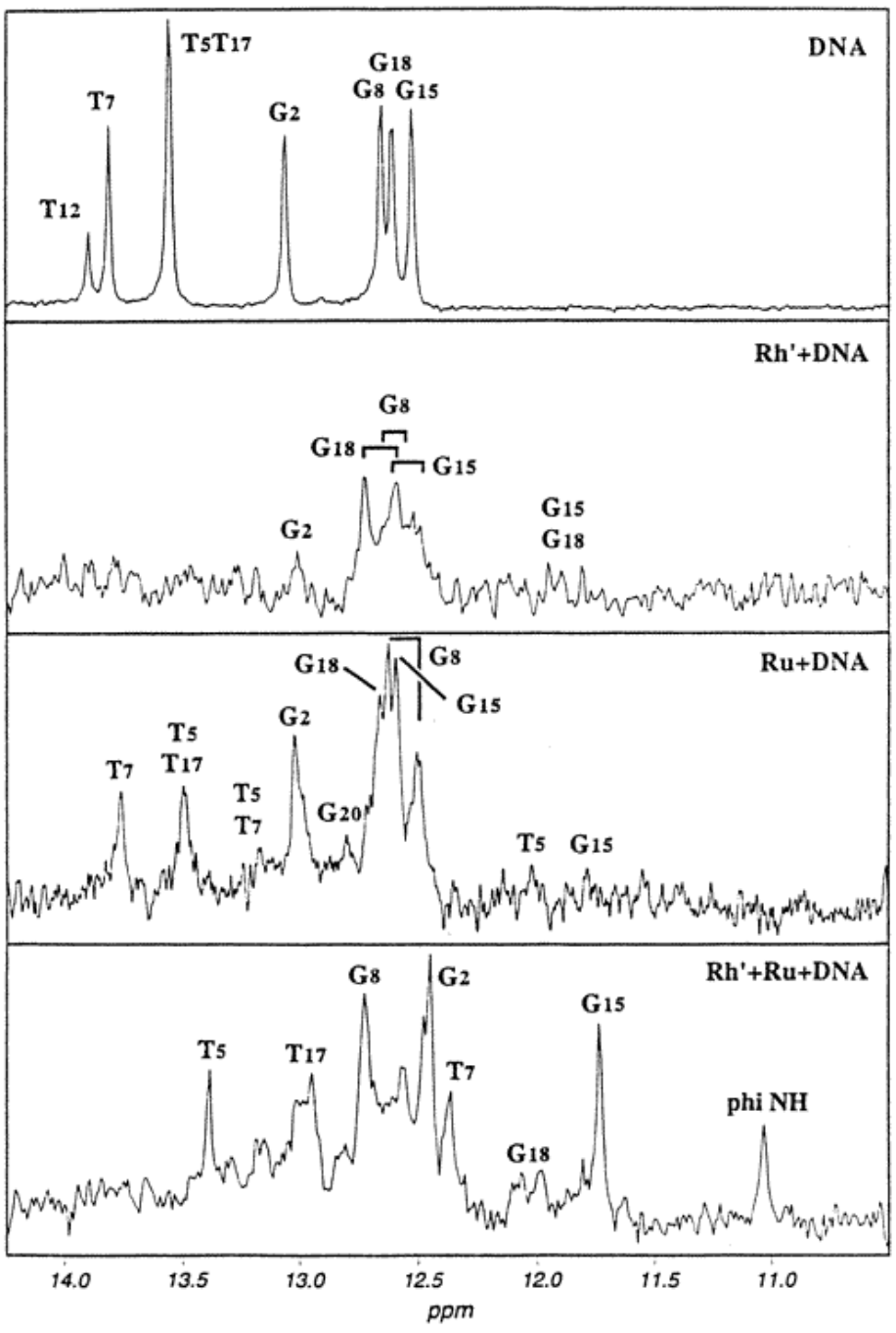

Figure 6.7 1-D ^{1}H NMR spectra in the imine region for in 90:10 H_2O/D_2O for (top to bottom) D1/D2 alone, Rh'+D1/D2, Ru+D1/D2, and Rh'+Ru+D1/D2.

particularly ill defined in the imine region (Figure 6.7), where the only large peaks are a cluster of G imine peaks around 12.6 ppm, near the original locations of G8, G18, and G15. There is also a very weak, broad peak at 11.8 ppm which may be either or both G18 and G15, but these cannot be distinguished conclusively from these data alone. The cytosine base fingerprint region (Figure 6.6), however, allows us to conclude that both G18/C3 and G15/C6 base pairs are significantly perturbed, while G8/C13 is not. Additionally, cross-peaks between T5 CH_3 and T17 CH_3 and aromatic protons are significantly broadened, indicating multiple chemical environments for these bases. This extensive broadening and the finding of perturbations to many of the resonances is consistent with photocleavage studies of site selectivity;[23] Rh' appears to be a fairly nonspecific metallointercalator, binding best on either side of both C19 and C6.

From these data, we may assign with confidence where the rhodium complex does *not* bind on the decamer. The nearly unchanged G8 imine peak (Figure 6.5) and the unperturbed C13 and C10 H5-H6 peaks (Figure 6.6) indicate that the Rh' metallointercalator avoids the 5'-$G_8A_9C_{10}$-3' end of the duplex.[35] Figure 6.8 illustrates this binding equilibrium. It should be noted that each methylene of the phen' arm produces one sharp peak in the spectrum. No interaction with DNA is apparent, as expected given the negative charge of the pendant carboxylate. The carboxylate arm therefore acts merely as an NMR marker.

NOESY Contour for Ru+DNA. The addition of Ru to D1/D2 yields a reasonably sharp ^{1}H NMR spectrum in 90:10 H_2O/D_2O which is broadened compared to that of the DNA alone but much less so than the Rh'+DNA spectrum.[36] The imine region of the Ru+DNA spectrum is much more informative than its Rh'+DNA counterpart. The imine peaks from 11–14 ppm are all reasonably sharp and approximately unchanged in chemical shift from their positions in the absence of metal complex. However, there are several cross-peaks which point toward the possibility of exchange of the ruthenium intercalator between two or more sites, in addition to exchange with the small excess of

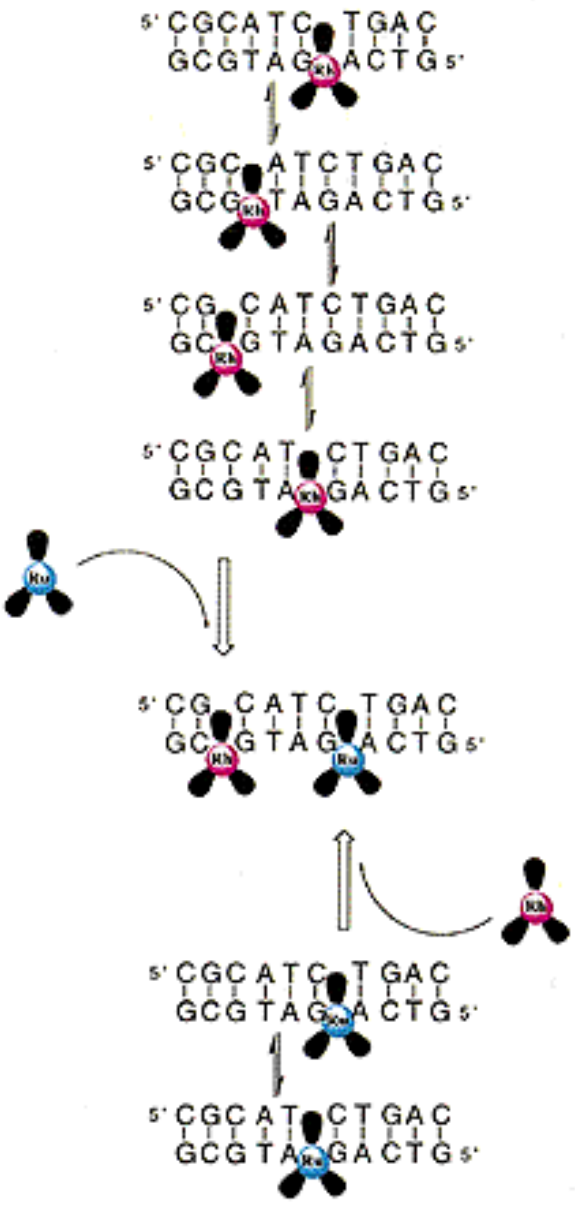

Figure 6.8 Schematic illustration depicting the sites occupied in the binding equilibria for Rh' and Ru intercalation separately and together in the DNA decamer.

free DNA. If we assume there are two nearly equal binding sites, there is approximately enough metal complex to half-fill each site; some population of unshifted protons will arise, even for a site of intercalation. As in the Rh'+DNA spectrum, there is a cluster of G imine peaks at approximately the original shift of G8, G18, and G15, but now with clear exchange peaks among one another, indicating pairs of shifts for each (Figure 6.5). The peak at the original shift for G15 now has cross-peaks to two upfield positions (at 11.55 ppm and 11.76 ppm); this indicates an upfield shift of -0.76 ppm and -0.97 ppm, respectively, for the bound sites. The G2 imine resonance is strong and predominantly unshifted from its uncomplexed location; cross-peaks upfield -0.3 ppm and -0.4 ppm are likely NOEs to G20 and G18. As evident in Figure 6.5, both T7 and (T5+T17) diagonal peaks are strong, but each shows upfield cross-peaks. T7 has a cross-peak at 13.16 ppm, upfield -0.65 ppm from its free DNA position. The coincident T5 and T17 imine peaks also have a cross-peak at 13.15 ppm, upfield -0.41 ppm. Additionally, there is a cross-peak upfield to 12.0 ppm, where the diagonal peak is weak and broad. The imine peak of T12 is absent, likely the result of fraying of the duplex ends.

The aromatic region and the C H5-H6 / C NH_2 fingerprint region (Figure 6.6) again show a pattern similar to that seen in the free DNA spectrum, but with some notable differences. In the C NH_2 region, C19 is very strong and unperturbed. The C13 region is little changed, though perhaps broadened compared to the spectrum for free DNA. The C6 resonance, in contrast, is much weaker and broadened, though only slightly changed in chemical shift. In the C H5-H6 region, a complementary pattern is seen. C1 is sharp and unchanged, as is the C19 resonance. C13 appears somewhat broad, though not as dramatically as C3 or C6, the latter being broadened almost completely.

Table 6.1 summarizes the shifts observed. These spectral changes, taken together, support the conclusion that Ru intercalates in the D1/D2 decamer centrally, fairly specifically, preferentially binding on either side of the C6/G15 base pair. More detailed conclusions regarding the intercalation cannot be drawn. This binding equilibrium,

which is illustrated in Figure 6.8, leads to significant upfield shifts of the T5 and T7 imino peaks and two upfield-broadened resonance positions for G15. Only slight perturbations of the G8 and G18 imino protons and C3 NH_2 protons are evident.

Imino proton	DNA	Rh'+DNA	Ru+DNA	Rh'+Ru+DNA
C1/G20	------	------	[12.8]	------
G2/C19	13.06	[13.01]	13.01	12.45
C3/G18	12.61	12.73, 12.60, [11.80]	12.72	12.73, 12.48, 12.05
A4/T17	13.56	[13.50]	13.50	13.01, 12.94
T5/A16	13.56	[13.50]	13.50, 13.15, 12.01	13.39
C6/G15	12.52	12.65, 12.50, [11.80]	12.50, 11.76, 11.55	[12.57], 11.74
T7/A14	13.81	13.81	13.76, 13.16	12.36
G8/G13	12.66	12.65, 12.55	12.63, 12.47	[12.69, 12.50]
A9/T12	13.90	[13.90]	------	13.85
C10/G11	------	------	------	------

Table 6.1 Chemical shifts (ppm) of the T and G imino protons of D1/D2 alone and with metal complexes.

NOESY Contour for Rh'+Ru+DNA. With the addition of both metallointercalators to the decamer, the spectrum becomes quite dense owing to the abundance of aromatic protons, but many resonances are clearly in slow exchange. In this spectrum the imine region (Figures 6.5 and 6.7) is sharpened significantly compared to that for either complex alone with DNA, and this enhanced resolution suggests either slower exchange kinetics or greater site selectivity for the two bound together versus separately. The Rh'+DNA and Ru+DNA spectra showed each of the complexes in

exchange between two or more sites, but the breadth and intensity of the peaks suggested no single site was predominantly filled. Here the stoichiometry is such that two sites can be essentially completely filled, either with metal complexes maintaining their lack of site specificity, exchanging between sites, or with each site being specifically occupied by one metal complex. The observation of sharp imine peaks, with very little exchange broadening evident, argues against two intercalation sites being occupied by the same metal complex but instead suggests that each metal complex may fill a specific site.

The imine region contains a series of sharp, well-defined resonances including a resonance near 11 ppm for the intercalated phi NH (Figure 6.7). An analogous intercalated phi peak is not evident in the Rh' only spectrum and supports the idea that Rh' binds with greater specificity to the decamer in the presence of Ru than in its absence. Inspection of the NOESY contour and Table 6.1 shows strong, highly shifted resonances for T7, G15, and G2, with upfield shifts of -1.45 ppm, -0.78 ppm, and -0.61 ppm respectively, consistent with adjacent intercalation. The imine/aromatic region of the 2-D plot shows C NH_2 connectivities to these upfield shifted G imino protons but not to the G18 or G8 imino position. The dramatic shift in the T7 imine resonance is accompanied by a -1.55 ppm upfield shift of A14H2, consistent with a large ring system such as dppz intercalating deeply neighboring this base pair. The T17 imine peak appears as two nearly identically shifted peaks at 13.01 ppm and 12.94 ppm (upfield -0.55 ppm and -0.62 ppm). Both T17 imino and A4H2 protons have NOEs to G18 imino locations, and there is an NOE between T5 and T17 imino protons. The shift of the bound T17 resonance is consistent with some intercalation neighboring this site. The breadth and multiplicity of this resonance as well as substantial broadening of G18 (based on the 2-D contour) suggests significant exchange from this site, in contrast to that between G18 and G2. In fact, the shifted T17 resonance appears more intense and complex than other peaks due to overlap of the free G2 resonance. Also noteworthy are imine resonances which vary little compared to that for the free DNA spectrum. The T5 imino proton is shifted only -0.17

ppm upfield, indicating no adjacent intercalation. The T12 imine peak is weak, but at the same resonance position as in the free DNA spectrum. The G8 peak is strong and unperturbed.

From these data we cannot definitively determine which metal complex binds to a given site, but only that a given base step has been perturbed by intercalation. We can infer, however, which site each complex occupies based on the magnitude of imine chemical shifts and the spectral comparison to the behavior of each complex independently. First, in comparing shifts for the Rh' only spectrum with the Ru only spectrum, it is apparent that the ruthenium intercalator may induce larger magnitude shifts with intercalation. On that basis, if we examine shifts in the imine region for the Rh'+Ru+DNA spectrum, we may ascribe intercalation neighboring G2 to Rh' and between G15-T7 to Ru. This assignment is fully consistent with the site preferences of each metallointercalator individually. We also see that the site specificity is enhanced on this basis.

Despite the enhanced resolution, the aromatic region begins to become cluttered with NOEs between the intercalated ligands of the metal complexes and DNA, and this makes the C H5-H6 peaks difficult to distinguish (Figure 6.6). Nonetheless, some distinct changes in these peaks are observed. The most obvious features of the C NH_2 fingerprint region are the new chemical shifts for C19 and C6 (upfield for the hydrogen-bonded C N*H*, downfield for C NH) and the enhanced sharpness of an unshifted C13. In fact, a NOE between C13N*H* and A9H8 can even be seen, which suggests this end of the duplex is more rigid and exchanging less than in the free DNA. The C NH_2 peaks of C10 and C1 are unchanged in location, though weak, and C3 is broadened.

In the complicated C H5-H6 region, a new location for a sharp C19 peak can be readily distinguished. The C H5-H6 peaks of C1 and C10 are strong and unshifted. The C13 peak is shifted slightly into a complicated region but can be identified from the

C H5-C NH cross-peak. The remaining cytosine bases, C6 and C3, have very broad C H5-H6 peaks, consistent with the behavior of their C NH_2 cross-peaks.[37]

These spectra are consistent with a model in which the two metallointercalators exhibit fairly specific binding toward either end of a decamer duplex, despite each individual complex preferring a more sequence neutral, central intercalation pattern. One complex, likely Ru based upon the shifts (*vide supra*), is binding between C6-T7, while the other complex intercalates primarily at G2-C3, with some exchange into C3-A4. Given the nearest neighbor exclusion principle governing intercalation into a DNA duplex[38,39] and strong intercalation into the C6-T7 interbase step, cooperative binding should correspond to intercalation of the other complex at the A4-T5 step or between G8 and A9.[39] In that case, either T12 or T5 imino protons would be shifted upfield. However, it is clear that both T12 and T5 are nearly unmoved, so the *nearest neighbor binding site is not occupied*.[15]

The 1-D NMR spectra of the imine regions of D1/D2 alone, Rh'+DNA, Ru+DNA, and Rh'+Ru+DNA (Figure 6.7) provide a basis for qualitatively comparing the site multiplicity and occupancy of sites. The assignments indicated are based on the 2-D data, where NOE cross-peaks clearly demonstrate the identity even of the weak and broad peaks. For the DNA duplex by itself, the imine peaks of the terminal base pairs are not observed, and T12 is attenuated due to the flexibility of the duplex ends. The remaining imine peaks are sharp and have integral areas. The spectrum of Rh'+DNA, in contrast, is quite broad. The occupancy of the sites cannot be estimated, but there are clearly multiple binding modes contributing to the exchange broadening. The spectrum of Ru+DNA is noticeably sharper than the Rh'+DNA spectrum, but the shifted peaks are again quite broad. In contrast to the two metallointercalators alone with DNA, the two together give distinct and sharp bound peaks. This is indicative of a lower number of sites occupied by each complex, and there is little exchange with unshifted positions. For the Rh' site (G2-G18), the strong G2 peak and broad but not weak G18 peak suggest that

this site is occupied the majority of the time. Some exchange may take place with the neighboring C3-A4 interbase position, based primarily upon the shift in the T17 imine resonance, but this shift is also consistent with the attenuated effect of intercalation one base pair away. Moreover, the intensity of the shifted T17 imino resonance is enhanced due to overlap of free G2. The intensity of bound G2, adjacent to the Rh' intercalation site, is comparable to G8, which is in an unbound region of the duplex. Similarly for the Ru site (C6-T7), the strong G15 and T7 imine peaks suggest this site is substantially occupied. In fact, G15 is also comparable in intensity to G8.

6.3.3 Binding of Ru and Rh' to the DNA decamer

Given that the metal complexes are rigid and that metallointercalation does not cause large perturbations in the DNA structure, one can examine the relative dimensions and positioning of the metal complexes on the helix based upon the intercalation sites determined from the imine proton shift data. Within this model, some variation of the orientation of the metal complexes in the site is possible. The relative orientation of the two intercalators, nonetheless, is also constrained by the winding of the helix. However, whether the dppz ligand of the Ru complex is intercalated straight on or canted, the closest contact between *ancillary* phen (Ru) and phi (Rh') ligands is about 11 Å (closest distance from ancillary phi-H to phen-H), with the metal centers separated by about 20 Å (Ru-Rh separation); the intercalated ligands lie 17 Å apart along the helix axis. For a smaller population of Rh' complex intercalated between C3 and A4, the metal complexes would be separated by 15 Å (aromatic-aromatic distance). We had proposed earlier that the fast, photoinduced electron transfer proceeded over an aromatic-aromatic distance ≥ 10 Å with no direct contact between ancillary ligands.[4] Direct contact of the ancillary ligands is not possible at these interbase pair separations, even with substantial canting of each metal complex toward one another on the DNA helix.[40]

It is evident that binding of one metallointercalator to the DNA does not promote cooperative, close binding of the other to a neighboring site. If anything, in the mixed-

metal system, the intercalators are stabilized at positions further from one another on the decamer. Rather than associating one with another on the helix, the complexes are bound distinctly away from one another in a manner consistent with anticooperative binding on the helix.[15] This anticooperative association would be fully consistent with expectations based upon charge repulsions between the two cationic complexes.

6.3.4 Time-resolved emission studies of photoinduced electron transfer on the DNA decamer

Shown in Figure 6.9 are the time-resolved luminescence decay traces for Ru bound to the decamer duplex D1/D2, the system studied by NMR, in the absence and presence of Rh'. As apparent in the Figure, given the noticeable decrease in I_0 (the intensity at zero time), static quenching occurs on a timescale which is fast compared to the instrument response time ($>10^9$ s^{-1}). Table 6.2 summarizes both time-resolved and steady-state luminescence data in the absence and presence of Rh as well as Rh'. As seen with all DNA polymers, time-resolved decays in emission are best described by a biexponential fit. We attribute this biexponential decay profile to the presence of families of intercalating geometries.[20,25] Similar percentage contributions of the lifetime components of Ru in the absence and presence of Rh' supports the notion that dynamic quenching plays little, if any, role in the loss of emission.

Equiv. Rh(III)	τ_1 (ns)	% τ_1	τ_2 (ns)	% τ_2	Fq
0	146 (1)	73	683 (1)	27	-----
1 Rh	131 (1)	72	628 (5)	28	0.62 (1)
1 Rh	116 (2)	76	538 (13)	24	0.74 (1)

Table 6.2 Time-resolved luminescence lifetimes and quenching values for the quenching of Ru fluorescence by Rh and Rh' in the presence of D1/D2.

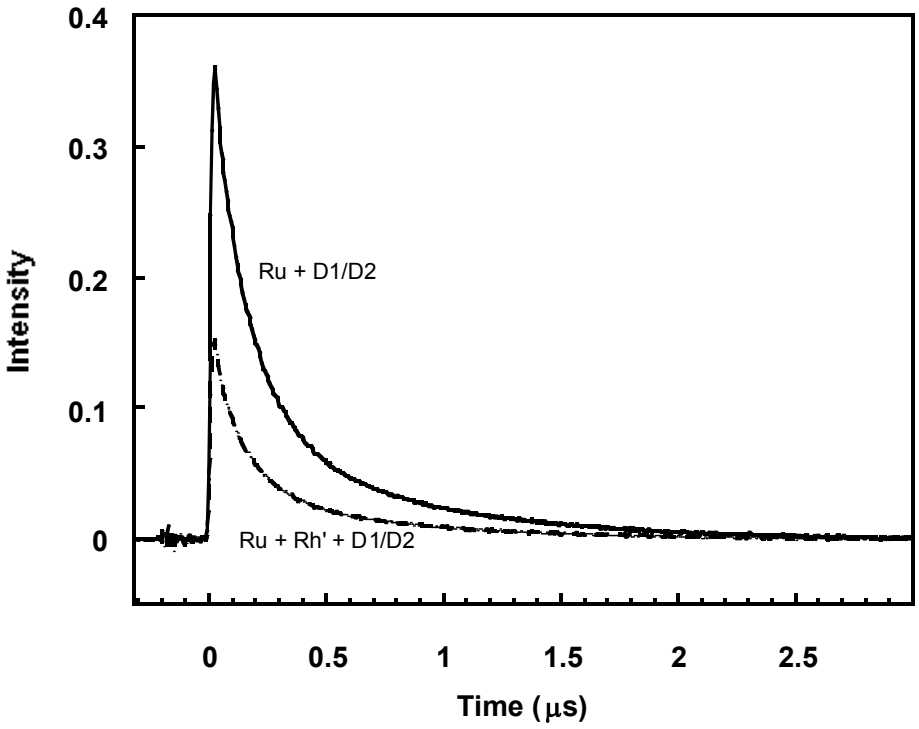

Figure 6.9 Time-resolved emission decay of photoexcited Ru (10 μM) bound to the DNA decamer D1/D2 (10 μM) in the absence (solid) and presence (dashed) of Rh' (10 μM) in 5 mM sodium phosphate, 50 mM NaCl, pH=7.2 buffer. Photoinduced quenching occurs on a fast time scale.

Integration of the luminescence decays from 0–3 μs reveals that the fraction quenched in the Ru/Rh' system is about 62%; steady-state measurements give a similar value. Quenching of Ru emission by Rh also occurs on a fast timescale and is slightly more efficient. This somewhat increased efficiency likely reflects the increased binding affinity of the rhodium intercalator of higher charge. Overall, the presence of the pendent phen' arm is inconsequential. The magnitude of the quenching may also be compared with the site occupancies evident by NMR. One might question why the emission is not quenched 100%. The intercalators exchange on the decamer on a timescale much slower

than is monitored in the luminescence quenching experiment. With intercalators noncovalently bound, some duplexes contain one Ru and one Rh, but others, albeit to a small extent based upon the NMR results, will contain two Ru's or two Rh's. Therefore, the quenching observed is fully consistent with efficient quenching on DNA polymers. Clustering of the metallointercalators at short range on the helix cannot account for this level of quenching. Importantly, electron transfer rates[4] of 10^{10} s^{-1} for the recombination reaction cannot be explained simply by invoking 5–10 Å through-space edge-edge proximity (not contact) of complexes intercalated at a three or four base pair separation on the helix. Rather, this amount of quenching requires fast, photoinduced electron transfer between separated Ru(II) and Rh(III) complexes mediated by the DNA base stack.

6.4 Conclusions

We have systematically reexamined the CD results reported[13] by Nordén and coworkers and find they are incomplete. This previous CD study had provided a new spectroscopic observation in support of clustering on the DNA helix by metallointercalators. We have looked at the change in CD intensity with added DNA for Rh only, Ru only and the two together at constant ratio. Titrations have been conducted for $[poly(dA\text{-}dT)]_2$, $[poly(dG\text{-}dC)]_2$, and calf thymus DNA. We find that the largest perturbations to the CD spectra occur upon the initial addition of DNA, consistent with a change in the chiral environment of each complex as they associate with the helical interbase pair site. There are subtle differences in the intensity of this induced CD dependent on the DNA sequence, which is consistent with the notion that it is the DNA binding environment, rather than a nearby metal complex, which affects the CD spectrum. No systematic change in CD as a function of loading on any of the DNA sequences is apparent. Moreover, the variation in CD intensity as a function of increasing Rh/Ru ratio shows no upward curvature and is linear at concentration ratios

where substantial luminescence quenching is observed. Therefore, *the CD results are not consistent with cooperative binding of the two metal complexes on a DNA polymer*. Association of the metallointercalator with the diastereomeric precipitating agent would account for the incomplete results reported previously, although studies in our laboratory have not been conducted using this diastereomeric salt.

In addition to the CD data, Nordén and coworkers presented luminescence quenching titrations at a series of P/Ru ratios and analyzed these quenching results according to several models. A cooperative clustering model with the high cooperativity parameter of $\omega_{Ru\text{-}Rh} = 55$ fit the data best over all loadings. A sphere-of-action model with quenching only of the nearest donor also fit the data well at the metal/DNA loadings (P/Ru = 100) where quenching studies had been carried out previously, and it is this model that to first order would be in line with a long-range electron transfer mechanism. In Nordén's experiments at higher loadings of both Ru and Rh, however, deviations in the data from the sphere-of-action model are evident. Based upon our experiments, these deviations could also reflect the technical difficulties associated with obtaining reliable data at high loadings where precipitation is an issue. In this concentration range, precipitation occurs because of significant charge neutralization of the DNA by the metal complexes, and the overall complex solubility should be decreased still more for the arsenyl tartrate salt. The uncertainty in measurement, not provided by Nordén, is additionally increased at the higher Rh concentrations, since the overall luminescence signal is *exceedingly* small. Within the concentration regime where data are reliable, both clustering and the model consistent with long-range electron transfer can be applied reasonably well in describing the quenching results of luminescence titrations. Certainly neither model can be ruled out based upon these data.

Barbara and coworkers also present their analysis of the spectral titrations of Δ-Ru bound to calf thymus DNA with Δ-Rh at low loading in terms of clustering. Here, using three adjustable parameters, a somewhat better fit is obtained with a clustering model

rather than a model incorporating long-range electron transfer with $\beta = 0.16$. Given the many parameters utilized as well as those not taken into account in luminescence quenching modeling (i.e., site preferences), again, certainly neither model can be ruled out on the basis of these fits alone. Instead the analysis suggested that other experimental studies were needed to distinguish between these models and better describe the system. In fact, no similar analyses were applied to the other titrations carried out using different ruthenium donors or DNA polynucleotide sequences, where the validity and generality of some of the parameters obtained could have been explored.

Importantly, both Nordén and Barbara fail to explain the basis for the large cooperative stabilization ($\geq$1.5 kcal/mol)[13,14] between the highly charged Ru and Rh intercalators but not between each individually that the fits to clustering models require. A clustering model is additionally difficult to visualize in structural terms given that efficient quenching is seen between Δ-Ru and Δ-Rh on both $[poly(dA\text{-}dT)]_2$ and $[poly(dG\text{-}dC)]_2$ but with significantly different rates (40 times greater for $[poly(dA\text{-}dT)]_2$).[4] If the fast electron transfer rates were the result of direct contact between donor and acceptor, one should expect similar rates of recombination (measured by transient absorption spectroscopy) irrespective of the DNA polymer. In fact, when the donor and acceptor are encouraged to cluster in SDS micelles, no fast luminescence quenching is observed.[7]

The question here with respect to DNA-mediated electron transfer actually is not a thermodynamic one but a structural one. Do the metal complexes contact each other, or does electron transfer occur at long range? It was for this reason that we also undertook a structural study, using NMR, to examine this question directly. The binding of Rh' and Ru metallointercalators to a non-self-complementary decamer duplex was examined using 2-D NMR methods. Binding sites of the metallointercalators individually and together on the DNA decamer were determined based primarily upon the characteristic upfield shifts of base pair imine peaks neighboring sites of intercalation. For each bound

individually, the NMR data are broad, reflective of exchange between multiple sites. The data suggest that Rh' intercalates in at least four sites but avoids the 5'-$G_8T_9C_{10}$-3' end of the duplex. Ru, in contrast, appears to bind adjacent to C6/G15, primarily at the C6-T7 interbase pair step. Interestingly, the spectra are sharpened with both metal complexes bound to the helix, consistent with a higher site selectivity for the two metals associated together on the duplex. The NMR data are consistent with the metals being associated with sites further toward the duplex ends than observed for each independently.

Fundamentally, the important observation is not that these bulky complexes bind near an end, but that they bind *away* from one another. These data certainly do not permit a high-resolution view of the metal complexes bound to DNA, but they do address directly their sites of binding on the helix. This binding is not associative but repulsive. The NMR experiment is not a measure of the energetics of association, but it addresses the structural question. The conclusion drawn must be that the complexes do not cluster on the helix. This structural conclusion is precisely that which eliminates short-range effects as an explanation for the observed rapid quenching. Our NMR results indicate anticooperative (repulsive) binding, leading primarily to a separation of four base pairs between intercalation sites. Moreover, time-resolved emission studies demonstrate that rapid quenching ($>10^9$ s^{-1}) of Ru emission occurs by Rh' bound to this decamer, under conditions where NMR data indicate that they are well separated.

From these data we conclude that the Rh(III) and Ru(II) intercalators do not cluster on a DNA helix. Importantly, therefore, the observed fast, photoinduced electron transfer between DNA-bound intercalators cannot be attributed to short-range contact.

Here we have shown, in a structural study, the noncovalent and noncooperative binding of two metallointercalators to specific, well-separated sites on a DNA decamer, and we have observed fast photoinduced electron transfer quenching between the bound complexes in this system. The rapid electron transfer we observe over >14 Å mediated by the DNA base pair stack is significant and remarkable. There have recently been

several efforts in the literature to discount long-range electron transfer through the DNA π stack as a viable mechanism because of clustering.[13,14,19] We have reported several significantly different studies using *covalently linked* intercalators in which clustering cannot provide an explanation for the observations made. We have demonstrated long-range charge transfer in reactions of metallointercalators with other metallointercalators,[3] with organic intercalators,[8,41] and with bases within the DNA stack.[10–12] The results reported here are fully consistent with those studies. Moreover the results described here show that clustering is not a viable model through which to view our prior results with noncovalently bound metallointercalators, nor certainly our results with covalently tethered intercalators. Nonetheless, we continue to maintain that a systematic investigation of DNA-mediated electron transfer as a function of distance should be undertaken only with covalently bound donors and acceptors.

6.5 References

1. Holmlin, R. E.; Dandliker, P. J.; Barton, J. K. *Angew. Chem.* **1997**, *36*, 2715.

2. (a) Stemp, E. D. A.; Barton, J. K. *Met. Ions Biol. Syst.* **1996**, *33*, 325. (b) Meade, T. J. *Met. Ions Biol. Syst.* **1996**, *32*, 453. (c) Beratan, D. N.; Priyadarshy, S.; Risser, S. M. *Chem. Biol.* **1997**, *4*, 3.

3. Murphy, C. J.; Arkin, M. R.; Jenkins, Y.; Ghatlia, N. D.; Bossmann, S.; Turro, N. J.; Barton, J. K. *Science* **1993**, *262*, 1025.

4. Arkin, M. R.; Stemp, E. D. A.; Holmlin, R. E.; Barton, J. K.; Hormann, A.; Olson, E. J. C.; Barbara, P. F. *Science* **1996**, *273*, 475.

5. (a) Holmlin, R. E.; Stemp, E. D. A.; Barton, J. K. *J. Am. Chem. Soc.* **1996**, *118*, 5236. (b) Stemp, E. D. A.; Arkin, M. R.; Barton, J. K. *J. Am. Chem. Soc.* **1995**, *117*, 2375.

6. Murphy, C. J.; Arkin, M. R.; Ghatlia, N. D.; Bossmann, S. H.; Turro, N. J.; Barton, J. K. *Proc. Natl. Acad. Sci. U.S.A.* **1994**, *91*, 5315.

7. Arkin, M. R., Stemp, E. D. A.; Turro, C.; Turro, N. J.; Barton, J. K. *J. Am. Chem. Soc.* **1996**, *118*, 2267.

8. Kelley, S. O.; Holmlin, R. E.; Stemp, E. D. A.; Barton, J. K. *J. Am. Chem. Soc.* **1997**, *119*, 9861.

9. O'Neill, P.; Fielden, E. M. *Adv. Radiat. Biol.* **1993**, *17*, 53.

10. (a) Hall, D. B.; Holmlin, R. E.; Barton, J. K. *Nature* **1996**, *382*, 731. (b) Hall, D. B.; Barton, J. K. *J. Am. Chem. Soc.* **1997**, *119*, 5045.

11. Arkin, M. R.; Stemp, E. D. A.; Pulver, S. C.; Barton, J. K. *Chem. Biol.* **1997**, *4*, 389.

12. (a) Dandliker, P. J.; Holmlin, R. E.; Barton, J. K. *Science* **1997**, *275*, 1465. (b) Dandliker, P. J.; Nuñéz, M. E.; Barton, J. K. *Biochemistry* **1998**, *37*, 6491.

13. Lincoln, P.; Tuite, E.; Nordén, B. *J. Am. Chem. Soc.* **1997**, *119*, 1454.

14. Olson, E. J. C.; Hu, D.; Hormann, A.; Barbara, P. F. *J. Phys. Chem.* **1997**, *101*, 299.

15. Clustering, or cooperative binding, thermodynamically represents the increased stabilization associated with intercalative binding in the presence of another intercalator bound at the nearest neighbor site compared to the stabilization in the absence of the nearest neighbor. Noncooperative binding indicates equal stabilization in the absence and presence of a nearest neighbor. Anticooperative binding indicates a destabilization in the presence of a nearest neighbor compared to that in its absence. Structurally, cooperative binding might allow possible contact between the favored nearest neighbors. Anticooperativity, while leading to correlated binding, that is the complexes statistically avoiding one another on the helix, would result in an increased separation between complexes compared to random occupation.

16. Winkler, J. R.; Gray, H. B. *Chem. Rev.* **1992**, *92*, 369.

17. (a) Priyadarshy, S.; Risser, S. M.; Beratan, D. N. *J. Phys. Chem.* **1996**, *100*, 17678. Other theoretical models may better describe our results, however. See: (b) Felts, A. K.; Pollard, W. T.; Friesner, R. A. *J. Phys. Chem.* **1995**, *99*, 2929. (c) Evenson, J. W.; Karplus, M. *Science* **1993**, *262*, 1247.

18. Meade, T. J.; Kayyem, J. F. *Angew. Chem., Int. Ed. Engl.* **1995**, *34*, 352.

19. Lewis, F. D.; Wu, T.; Zhang, Y.; Letsinger, R. L.; Greenfield, S. R.; Wasielewski, M. R. *Science* **1997**, *277*, 673.

20. (a) Dupureur, C. M.; Barton, J. K. *J. Am. Chem. Soc.* **1994**, *116*, 10286. (b) Dupureur, C. M.; Barton, J. K. *Inorg. Chem.* **1997**, *36*, 33.

21. (a) David, S. S.; Barton, J. K. *J. Am. Chem. Soc.* **1993**, *115*, 2984. (b) Hudson, B. P.; Dupureur, C. M.; Barton, J. K. *J. Am. Chem. Soc.* **1995**, *117*, 9379. (c) Hudson, B. P.; Barton, J. K. *J. Am. Chem. Soc.* **1998**, *120*, 6877.

22. Amouyal, E.; Homsi, A.; Chambron, J.-C.; Sauvage, J.-P. *J. Chem. Soc., Dalton Trans.* **1990**, 1841.

23. (a) Pyle, A. M.; Chiang, M. Y.; Barton, J. K. *Inorg. Chem.* **1990**, *29*, 4487. (b) Sardesai, N. Y.; Lin, S. C.; Zimmermann, K.; Barton, J. K. *Bioconjugate Chem*. **1995**, *6*, 302. (c) Sitlani, A.; Barton, J. K. *Biochem.* **1994**, *33*, 12100.

24. Yoshikawa, Y.; Yamasaki, K. *Coord. Chem. Rev.* **1979**, *28*, 205.

25. (a) Friedman, A. E.; Chambron, J.-C.; Sauvage, J.-P.; Turro, N. J.; Barton, J. K. *J. Am. Chem. Soc.* **1990**, *112*, 4960. (b) Jenkins, Y.; Friedman, A. E.; Turro, N. J.; Barton, J. K. *Biochemistry* **1992**, *31*, 10809. (c) Hartshorn, R. M.; Barton, J. K. *J. Am. Chem. Soc.* **1992**, *114*, 5919.

26. Friedman, A. E.; Kumar, C. V.; Turro, N. J.; Barton, J. K. *Nucleic Acids. Res.* **1991**, *19*, 2595.

27. Piotto, M.; Saudek, V.; Sklenar, V. *J. Biomol. NMR* **1992**, *2*, 661.

28. Cooperative binding with site specificity was demonstrated in the case of Δ-$[Rh(diphenylbpy)_2phi]^{3+}$. This cooperativity depended upon the presence of the hydrophobic phenyl substituents. See: Sitlani, A.; Dupureur, C. M.; Barton, J. K. *J. Am. Chem. Soc*. **1993**, *115*, 12589.

29. (a) Mason, S. F.; McCaffery, A. J. *Nature* **1964**, *204*, 468. (b) Blake, A.; Peacocke, A. R. *Biopolymers* **1966**, *4*, 1091. (c) Gardner, B. J.; Mason, S. F. *Biopolymers* **1967**, *5*, 79. (d) Blake, A.; Peacocke, A. R. *Biopolymers* **1967**, *5*, 383. (e) Blake, A.; Peacocke, A. R. *Biopolymers* **1967**, *5*, 871. (f) Yamaoka, K.; Resnik, R. *Nature* **1967**, *213*, 1031. (g) Crothers, D. M.; Li, H. J. *Biopolymers* **1969**, *8*, 217.

30. Holmlin, R. E.; Stemp, E. D. A.; Barton, J. K. *Inorg. Chem.* **1998**, *37*, 29.

31. Ewing, A. R. *J. Chem. Soc.* **1985**, *67*, 102.

32. Wilson, W. D.; Li, Y.; Veal, J. M. *Advances in DNA Sequence Specific Agents*, JAI Press: Greenwich, CT, 1992; Vol. 1.

33. (a) Patel, D. J.; Shen, C. *Proc. Natl. Acad. Sci. U.S.A.* **1978**, *75*, 2553. (b) Feigon, J.; Denny, W. A.; Leupin, W.; Kearns, D. R. *J. Med. Chem.* **1984**, 450. (c) Searle, M. *Prog. Nucl. Magn. Reson. Spectrosc.* **1993**, *25*, 403.

34. Wüthrich, K. *NMR of Proteins and Nucleic Acids*; Wiley-Interscience: New York, 1986; Chapter 13.

35. As in the decamer alone, C10 NH_2 is not observed, due to its greater solvent accessibility as the terminal base.

36. This is also readily apparent in the region of the T CH_3 to aromatic cross-peaks.

37. The cross-peaks between T CH_3 groups and aromatic H6 and H8 protons are also informative about the structure of the decamer with two metallointercalators.

38. Crothers, D. M. *Biopolymers* **1968**, *6*, 575.

39. This nearest neighbor exclusion principle leads us to define cooperative binding as a two base pair separation between intercalating ligands, and noncooperative binding as a three or greater base pair separation.

40. For the major population with a four base pair separation between complexes, the closest distances between protons on the ancillary ligands range from 13–14 Å. For the minor population at a three base pair separation, the closest distances between protons on the ancillary ligands range from 7–8 Å.

41. Kelley, S. O.; Barton, J. K. *Chem. Biol.* **1998**, *8*, 413.